Rising dynamics and lift effect in dense segregating granular flows

Lydie Staron

View Online   Export Citation   CrossMark

ARTICLES YOU MAY BE INTERESTED IN

Dense granular flow of mixtures of spheres and dumbbells down a rough inclined plane: Segregation and rheology
Physics of Fluids **31**, 023304 (2019); https://doi.org/10.1063/1.5082355

Collapse of submerged granular columns in loose packing: Experiment and two-phase flow simulation
Physics of Fluids **30**, 123307 (2018); https://doi.org/10.1063/1.5050994

Rheology of binary granular mixtures in the dense flow regime
Physics of Fluids **23**, 113302 (2011); https://doi.org/10.1063/1.3653276

AIP Publishing

30, 123303

Rising dynamics and lift effect in dense segregating granular flows

Lydie Staron

Sorbonne Université, CNRS, Institut Jean Le Rond d'Alembert, F-75005 Paris, France

In order to explore the rising dynamics and the existence of a lift effect in dense segregating granular flows, we perform two-dimensional discrete numerical simulations in the case of single free intruders and bi-disperse granular mixtures. In both configurations, we do not observe a measurable lift force acting on the larger grains. The large force fluctuations acting on the bigger grains reduce to the weight of the latter, following the mere action-reaction principle. This suggests that the rising dynamics is driven by the force fluctuations, coupled with the properties of the surrounding granular bed itself. We propose the strong asymmetry displayed by granular bed resistance to downward (plunging) and upward (withdrawing) motion, as reported in detail by Hill *et al.* ["Scaling vertical drag forces in granular media," Europhys. Lett. **72**(1), 137–143 (2005)], as a key ingredient for segregation. Accordingly, moving an object toward the free surface is about 10 times easier than moving an object toward the rigid bottom. This asymmetry allows for an effective upward motion when large grains are submitted to upward force fluctuations, without being counterweighted by sinking episodes when large grains are submitted to downward force fluctuations. In addition to gravity, the existence of two different boundary conditions formed by the free surface and the rigid bottom explains this difference of resistance to motion. In this respect, the mechanism allowing size segregation in dense granular flows would be the same as that allowing legged locomotion in sand [Li *et al.*, "A terradynamics of legged locomotion on granular media," Science **339**, 1408–1412 (2013)]. *Published by AIP Publishing.* https://doi.org/10.1063/1.5045576

I. INTRODUCTION

In their natural occurrence, granular flows rarely exhibit the well-defined unique grain size so very useful in laboratory experiments or simulations for constraining granular flow behavior. On the contrary, they usually display a wide range of sizes, which may cover several orders of magnitude in extreme cases (as for debris or rock flows).[1–4] Even sand dunes, one natural granular system closest to its laboratory counterpart, are made of smaller and larger grains.[5]

An immediate consequence of the diversity of grain sizes is their sorting: while flowing or being shaken, large grains and smaller grains separate, forming specific patterns and thereby affecting the system evolution. In natural cases such as rock or debris flows, large grains rise to the free surface where they acquire a larger velocity. They accumulate at the front where they are pushed sideways by the advancing bulk, thus ending up forming levées that confine and channel the flow.[6–9] In geotechnical application, the separation by grain size may undermine the mechanical quality of concrete, or simply of a given soil. Grain size segregation, as the phenomenon is called, is thus a fundamental aspect of granular behavior. Yet, although a seemingly simple mechanism and in spite of the effort devoted to it, the mechanical origin of size segregation in dense granular flows remains elusive.

First attempts at describing size segregation essentially focused on the probability of large/small grains to migrate in the flow following a percolation-like picture of the phenomena, relying on the geometrical characterisation of the voids opening in a sheared flow as sites that smaller grains can occupy; the concept of "squeeze expulsion" explains why a large grain at the bottom starts to migrate upwards in the first place.[10–15] A mechanical explanation for grain size segregation was introduced later by Gray and Thornton.[16] In this model, segregation is understood as resulting from the heterogeneous force transmission typically observed in granular packings of same-size grains and generalised to polydisperse (many-size) packings.[17–19] Accordingly, pressure partition in the media differs from the classical mixture theory: larger grains sustain a larger part of the mean pressure than prescribed by their volume fraction. This causes them to see larger gravity-induced pressure gradients and to rise as a result. This model allows for the successful description of gravity-induced segregation patterns by solving shallow-layer equations in a wide range of configurations.[9,20–22] The mechanical origin assumed (namely, non-classical pressure partition) is however difficult to establish,[23–26] although considering temperature gradients as in granular gas may provide a theoretical basis.[27] It is, beside, uneasy to translate in terms of a Lagrangian description of the dynamics of a given segregated particle. In this perspective, enlightening experiments were performed with the aim of quantifying the forces (namely, lift and drag forces) acting on intruders moving in granular media.[28–31] In these experiments, an intruder buried in a granular bed at a given depth is submitted to a slow motion (either a slow rotation or a slow drag) while its vertical position is constrained, and the forces exerted on it are measured. All report the existence of a lift force, either dependent on the pressure/depth[28] or independent of it.[30,31] In all cases, however, the intruder has a symmetrical shape so that

the asymmetry necessary to create a lift effect must originate from the granular bed itself. Applying discrete simulations, Guillard et al.[32] measured the lift forces acting on an intruder and identified precisely the role of both pressure and shear gradients. Recently, similar simulations of intruders constrained in height in a granular flow led to the interpretation of the lift effect as an equivalent of the Saffman effect in viscous-inertial flows.[33]

These intruder experiments are all performed for intruders whose position is constrained in the direction normal to the flow, either attached to a spring or simply a fixed point. Hence they cannot move freely in response to the application of a force. In segregating flows, however, things are different as the intruder can move freely; lift forces may thus relax and therefore may not build up to such high values, as observed in Refs. 30 and 32. The direct quantification of lift forces in freely segregating granular flows seems hardly feasible experimentally, as it would imply measuring the position of and the resulting force acting on a given entirely free intruder (not to say many intruders). Discrete numerical simulations, on the other hand, give access to all contact forces in a given flow, thus allowing direct computation of the resulting force on free intruders, as well as the easy exploration of the experiments parameters, as in Refs. 32–39. The identification of the mechanism leading to the rising of larger grains in freely segregating granular flows, applying discrete numerical simulation, forms the aim of the present paper. Note that we limit our study to the case of dense systems.

In the following, we present two-dimensional discrete numerical simulations of bi-disperse (two grain sizes) dense granular flows applying the contact dynamics (CD) algorithm.[40,41] The segregation of a single large grain (namely, an intruder) and the segregation of a collection of large grains are investigated in terms of the average force resultant applied to the large grains. In contrast to Refs. 32 and 33 for constrained intruders, we do not measure the existence of a net lift force. On the contrary, we find that contact forces applied to larger grains exhibit important fluctuations, but do on average balance the large grain weight following a simple action/reaction principle. We argue that the rising motion of the large grains is dominated by these large force fluctuations and is made possible by the strong asymmetry displayed by granular bed resistance to downward (plunging) and upward (withdrawing) motion, as reported in detail in Refs. 42–45. Following these authors, moving an object toward the free surface is about 10 times easier than moving an object toward the rigid bottom. This asymmetry allows for an effective rising dynamics when large grains are submitted to large positive (upward) forces without being counterweighted by equivalent sinking episodes when large grains are submitted to equivalently large negative (downward) forces.

The numerical techniques are briefly presented in Sec. II. The case of the single large intruder is discussed in Sec. III, while Sec. IV reports the case of bi-disperse granular mixtures. A discussion follows in Sec. V.

II. CONTACT DYNAMICS SIMULATIONS OF BI-DISPERSE GRANULAR FLOWS

The numerical method applied to simulate the granular flows is the Contact Dynamics (CD) algorithm,[17,40,41] already applied for segregation problems by the same author in Refs. 26 and 38. The basic ingredients of this method are the following. Grains interact at contacts through solid friction and hardcore repulsion. Solid friction imposes that locally, and the normal and tangential contact forces satisfy $f_t \leq \mu f_n$, where μ is the coefficient of friction at contact. Moreover, a coefficient of restitution e sets the amount of energy dissipated in collisions. The numerical values of μ and e affect the effective frictional properties of the flow (velocity, angle of repose. . .), but we do not consider their influence on the segregation process. Their value was set to $\mu = 0.5$ and $e = 0.5$, for all contacts irrespective of the size of the grains involved, and was not varied. The hardcore repulsion ensures that grains at contacts do not overlap beyond an accepted small δ that allows for contact detection. By contrast with Molecular Dynamics (MD) methods which introduce an explicit stiffness to describe the contact rigidity, the hardcore repulsion in the CD method is a non-smooth strict condition. The difference between MD and CD methods is however expected to be virtually null in the flow configuration studied, provided that both are used within the range of numerical parameters in which their validity is ensured.

Two-dimensional granular beds were simulated, formed of small grains of diameter d, and large grains of diameter D. To prevent the geometrical ordering likely to happen in 2D for strictly mono-sized packings, small grain diameter exhibits a variability of $\simeq 30\%$ in the single intruder configuration (namely, $0.044 \leq d \leq 0.06$). The dimensions of the granular bed are $L = 100d$ and $H \in [55d, 70d]$ (depending on the composition), with periodic boundary conditions in the direction of the flow. The basal boundary is made of a row of fixed grains of diameter 0.05 (namely, $\simeq d$). The mass density of the intruder/large grains is the same as that of the surrounding smaller grains ($\rho = 0.1$ kg m^{-2}).

Two configurations are considered. In the case of the single intruder, one large grain is buried in a bed of smaller grains inclined at a slope θ. While the flow develops (in a steady regime), the intruder rises from its initial position $H/3$ to the free surface. In the case of the granular mixture, small and large grains are initially deposited under gravity in a mixed state, achieved by random positioning of small and large grains

TABLE I. Summary of simulations performed.

Simulations	Volume fraction of large beads Φ_L	Slope θ (deg)	Grain size ratio D/d	Number of independent runs
Intruder	. . .	20, 21.5, 23	1.5, 2, 2.5, 3, 3.5, 4, 4.5, 5	144
Mixture	0.2, 0.4, 0.6 ($\pm$0.02)	20, 21.5, 23	1.5, 2, 2.5, 3, 3.5, 4, 4.5, 5	72

prior to deposition. As the flow develops at slope angle θ, the large grains rise in the flow. For all cases, contact forces, grains position, and velocity are computed and known. Simulations were performed varying the grain size ratio D/d from 1.5 to 5, the volume fraction of large grains Φ_L from 0.2 to 0.6 (in the case of mixtures), and the slope from 20° to 23°, as summarised in Table I.

III. SINGLE LARGE INTRUDERS

A single large intruder carried along by a flow of smaller grains forms a specific case of segregation, as it relies only on interactions with a uniform granular matrix, without resorting to cooperative mechanisms with fellow big grains. For this reason, it offers an interesting insight into the nature of the forces exerted by a flow of small grains on bigger objects, as a starting point to understand the dynamics of segregation.

In the following, we thus consider a single large grain initially buried in a bed of smaller grains allowed to flow under gravity at an angle θ (for which a stationary regime is reached). The intruder is left free to move along with the mass of smaller grains, namely, none of its degree of freedom is suppressed. Accordingly, its vertical position evolves in time in response to the forces exerted by the smaller grains on it. Discrete numerical simulations give us access to all contact forces so that we can accurately follow the resulting force acting on the intruder and explore the existence of a lift force.

A. Rising dynamics

We consider granular beds of width $L = 100d$, and height $H \simeq 60d$, made of small grains of mean diameter $d = 0.052$ m (uniformly distributed between 0.044 and 0.06) (see Fig. 1). A large intruder of diameter D is buried in the granular bed at an initial vertical position $H/3$. The intruder diameter D is alternatively $D = 1.5d$, $2d$, $2.5d$, $3d$, $3.5d$, $4d$, $4.5d$, and $5d$. The granular bed is tilted at an angle θ for which a stationary flow develops ($\theta = 20°$, 21.5°, and 23°). The duration of the simulations is set to 500 s, for which nearly all intruders eventually reach the free surface (but for two cases with D = 1.5d). For each value of D and θ, 5 to 10 independent runs are performed (for a total of 144 independent simulations).

FIG. 2. Vertical position of the intruder z_I (normalised by d) as a function of time for $D/d = 1.5$ for a slope angle $\theta = 23°$ and $D/d = 4$ for a slope angle $\theta = 20°$. The horizontal dashed line shows the averaged position of the free surface.

As a result of the flow, the intruder moves up and down. Its instantaneous vertical position z_I is recorded in the course of time. Figure 1(c) shows the case of an intruder with $D/d = 3.5$: we observe a fluctuating motion which eventually leads to the free surface. In less favorable cases, as shown in Fig. 2, the intruder reaching the free surface may be sucked down again in the bulk (here for $D/d = 4$), or its motion may exhibit larger fluctuations which impede the segregation process (for $D/d = 1.5$, for instance). These sinking episodes are reminiscent of the diffusive mechanisms described in Ref. 47 and leading to remixing. However, eventually, most intruders are segregated by the flow for the simulation duration considered.

The instantaneous resultant vertical force $f_{z,I}(t)$ resulting from all the intruder contacts with their neighbours is defined as

$$f_{z,I}(t) = \sum_{\alpha=1}^{n_I^\alpha} \vec{f_I^\alpha}(t).\vec{z},\tag{1}$$

where n_I^α is the number of contacts in which the intruder is involved at time t and $\vec{f_I^\alpha}$ is the force transmitted at the contact α. The example displayed in Fig. 1(c) ($D/d = 3.5$) shows that $f_{z,I}(t)$ undergoes large fluctuations. These force fluctuations do exist for all the simulations performed and for all size ratios D/d. They can reach above 60× the intruder weight and are generally of large amplitude. Their role in the rising dynamics is thus expected to be important.
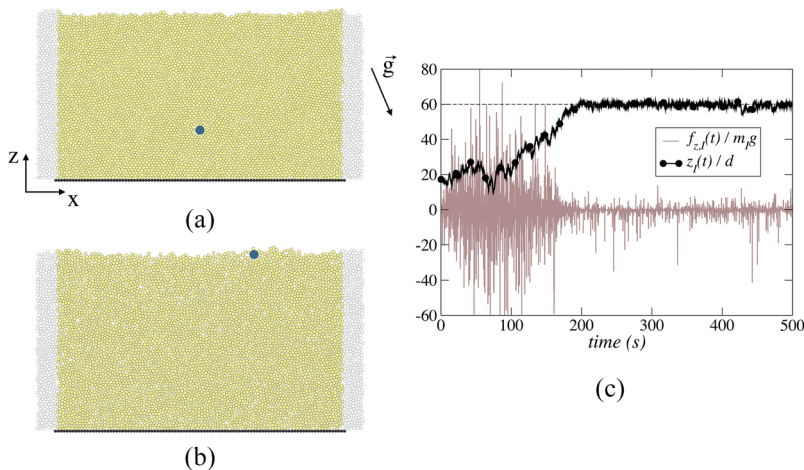

FIG. 1. An intruder of diameter D is initially buried in a bed of grains of diameter d [panel (a)]; as the flow develops at slope angle θ as a result of gravity, the intruder rises to the free surface [panel (b)]. The intruder vertical position and the vertical force resultant exerted on it evolve in time as shown in (c); the horizontal dashed line shows the averaged position of the free surface. In this example, $D/d = 3$ and $\theta = 23°$.

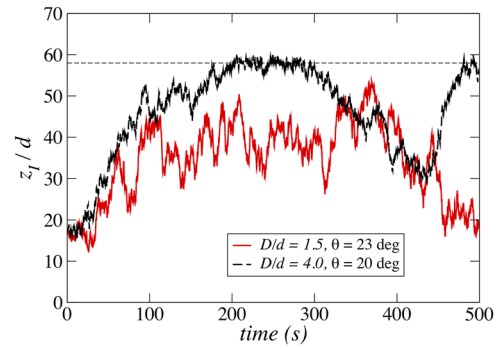## B. Forces applied to the intruder

We probe the existence of a lift force by simply averaging the instantaneous vertical force on the intruder $f_{z,I}(t)$ over the duration of the simulation,

$$F_I = \frac{1}{N_t} \sum_{t=1}^{N_t} f_{z,I}(t), \qquad (2)$$

with $f_{z,I}$ defined in (1). The dependence of F_I (normalised by $m_s g \cos\theta$, $m_s = \rho\pi d^2/4$) with the intruder size D (normalised by d) is shown in Fig. 3. For each pair (D/d, θ), the mean value averaged over all the independent runs is shown; error bars indicate the range of results over all the independent runs. We have moreover included the case $D/d = 1$. For a given value of D/d and θ, simulation results are scattered. Nevertheless we observe

$$F_I \simeq \cos\theta \, \rho\pi \frac{D^2}{4} g, \qquad (3)$$

namely, the averaged contact forces applied by the small grains on the intruder seem to be merely balancing the intruder weight, following the action-reaction principle (as was observed in numerical simulations of same size granular flows in Ref. 48). No additional positive contribution allows us for the identification of a net lift force, by contrast with Ref. 32. This means that if a lift force builds up, it is nearly entirely balanced by the drag induced by the intruder rising motion, and the net upward contribution is very small compared to the intruder weight and compared to the force fluctuations. This is not surprising in view of the typical rising dynamics displayed in Fig. 1(c). In this example, it takes about 200 s for the intruder to cover a distance of about $50d$ and reach the free surface, namely, a nearly zero acceleration. On the contrary, a sustained measurable lift force would send the intruder very quickly to the surface, a case never observed in our simulations.

On the other hand, the force fluctuations seen by the intruder are very important. It seems reasonable to suppose that these fluctuations, rather than a very small lift force, are dominating the intruder dynamics. We may suppose that over short time intervals, when upward/positive force fluctuations become much higher than the typical reaction to the weight of the intruder, the upward motion of the latter is made possible. The accumulation of such upward jumps results in the rising motion of the intruder.

On average, however, the vertical force resultant reduces to the intruder weight. Accordingly, the negative/downward force fluctuations do balance the positive ones. Although we observe the intermittent downward motion of the intruder, its amplitude does not counterweight the upward motion. In other words, while the upward and downward force resultants on the intruder are symmetrical, their effect in terms of motion is not.

We propose that this asymmetry proceeds from the fact that the resistance of a granular bed to an intruder motion is strongly dependent on whether the motion is upward or downward, even at important depths. This asymmetry was evidenced in Refs. 42–45, where intruders of different sizes and shapes were alternatively plunged or withdrawn from a static granular bed. It shows that for intruders of different shapes (including spherical), the force necessary for plunging the intruder in a granular bed (with no lateral confinement) is one order of magnitude larger than the force necessary for withdrawing it. This can be explained by the asymmetry created by the gravity gradient (as identified by Refs. 31 and 32) and, above all, by the different boundary conditions formed by the free surface on the one hand and the rigid bottom on the other hand, studied in detail in Ref. 44. In the context of the present simulation, this asymmetry is enough to account for the rising dynamics of the intruder without the contribution of a net lift force. In this scenario, the agitation, or "temperature," induced by the flow, generates large force fluctuations on the intruder, which is thereby allowed to explore both upward and downward motion in the packing and meeting much less resistance in the first case.

It would be of great interest to quantify precisely how resistance to motion itself is affected by the intruder size. The results in Ref. 42 report smaller resistance for larger intruders and a discrepancy between upward and downward motion increasing with the intruder size, which would imply that larger intruders tend to segregate better.

In a fluid-like picture of granular flows, it could be relevant to use an equivalent buoyant force instead of the simple weight of the intruder.[33] However, this would require the computation of the local solid fraction around the intruder, which depends strongly on the size ratio through the Voronoi calculation. This would introduce a geometrical bias in the analysis of our results and compromise their interpretation, the size ratio being an independent parameter of our study. Hence, we prefer the straightforward comparison with gravity forces, as in Ref. 32.

It is worthy to note that attempts at varying the time window over which F_I is computed (for instance, considering the rising dynamics only and filtering out time spent at the free surface) did not change the results in a significant way. At any rate, it did not help disclosing a different trend with the intruder size.

Finally, computing the relative velocity in the flow direction between the intruder and the smaller grains at the same height showed the existence of very small lags of fluctuating sign so that the analysis in terms of a viscous-inertial Saffman effect[33] seems not relevant here.
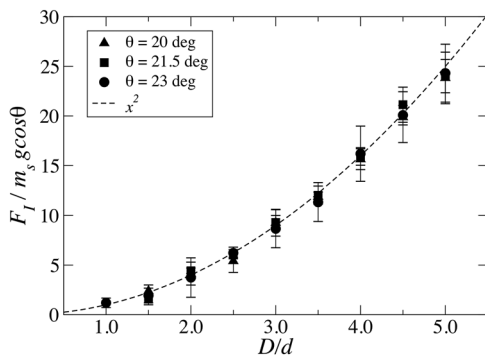
FIG. 3. Time-averaged vertical force resultant on the intruder F_I (normalised by the projected weight of a small grain $m_s g \cos\theta$) as a function of the normalised intruder diameter D/d for different slopes. The error bars are showing the range of results for all independent simulations. We observe that the vertical force exerted on the intruder balances its weight.
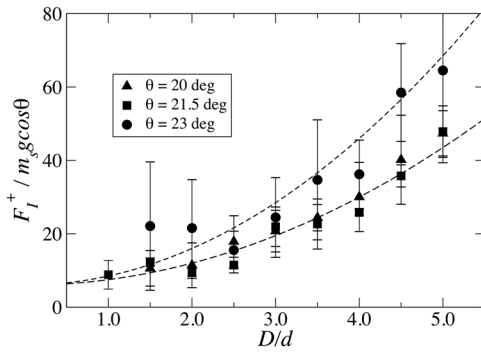
FIG. 4. Positive contribution F_I^+ of the time-averaged vertical force resultant on the intruder F_I (normalised by the projected weight of a small grain $m_s g \cos \theta$) as a function of the normalised intruder diameter D/d for different slopes. The error bars are showing the range of results for all independent simulations. The dotted lines show quadratic fits.

C. Focusing on upward force fluctuations

The rising motion results from a succession of upward jumps, presumably occurring when the resulting vertical force on the intruder undergoes a large positive fluctuation. Hence, we focus now on the positive values of $f_{z,I}$,

$$F_I^+ = \frac{\sum_{t=1}^{N_t} \mathcal{H}(f_{z,I}) f_{z,I}}{\sum_{t=1}^{N_t} \mathcal{H}(f_{z,I})}, \quad (4)$$

where $\mathcal{H}$ is the Heaviside function and the summation is made over all the time steps t of the simulation. We compute F_I^+ for all 96 independent simulations with D/d varying between 1 and 5 and the slope θ alternatively set to 20°, 21.5°, and 23°. The results are presented in Fig. 4, where $F_I^+/(m_s g \cos \theta)$ is plotted as a function of the size ratio D/d ($m_s = \rho \pi d^2/4$). We observe that the value of F_I^+ is scattered for larger values of θ, i.e., for very dynamical flows (e.g., $\theta = 23°$). For slower flows ($\theta = 20°$ and $\theta = 21.5°$), F_I^+ follows a clearer trend. In all cases, quadratic fits are acceptable,

$$\frac{F_I^+}{m_s g \cos \theta} \simeq \lambda_I \left(\frac{D}{d} \right)^2 + C, \quad (5)$$

where $\lambda_I \simeq 1.5$ for $\theta = 20°$ and $\theta = 21.5°$, $\lambda_I \simeq 2.5$ for $\theta = 23°$, and $C \simeq 6$ for all slopes investigated.

Essentially, F_I^+ scales like buoyancy forces, as observed in Ref. 32. Larger intruders are pushed upwards with a force increasing with their weight, giving them more power to displace the smaller grains covering them. Smaller intruders, including the grains forming the granular bed, also see large forces pushing them intermittently toward the free surface. But in these cases, segregation is less (or not) efficient, namely, the rising motion is counterbalanced by sinking episodes.

IV. BI-DISPERSE MIXTURES

A single intruder rises in a granular bed uniform in composition, and the system thus formed is accurately described by the knowledge of the intruder diameter D and that of the smaller grains forming the granular bed d. In a bi-disperse mixture, each large grain can be seen as an intruder, yet moving through a matrix of varying composition and undergoing forces from contacts with both small and large grains. While it flows, the granular bed changes geometry as each large grain tends to rise at the surface in a highly transient dynamics. Hence, we no longer speak of "intruders," but of the phase of large grains and the phase of small grains.

A. Rising dynamics

The systems studied are formed by a mixture of small grains (diameter $d = 0.04$) and large grains (diameter D) initially in a mixed state, as shown in panel 5. The volume fraction of large grains Φ_L may take the values 0.2, 0.4, or 0.6 (± 0.02), and the large grain diameter is alternatively set to $1.5d$, $2d$, $2.5d$, $3d$, $3.5d$, $4d$, $4.5d$, and $5d$, as in the case of the single intruder. The systems thus formed are tilted at an angle θ for which they develop into steady flows ($\theta = 20°$, $21.5°$, and $23°$). As a result, the initially well-mixed phases of large grains and small grains separate, with the larger grains rising at the surface, as shown in Fig. 5. A total of 72 independent runs are performed.

(a)   (b)
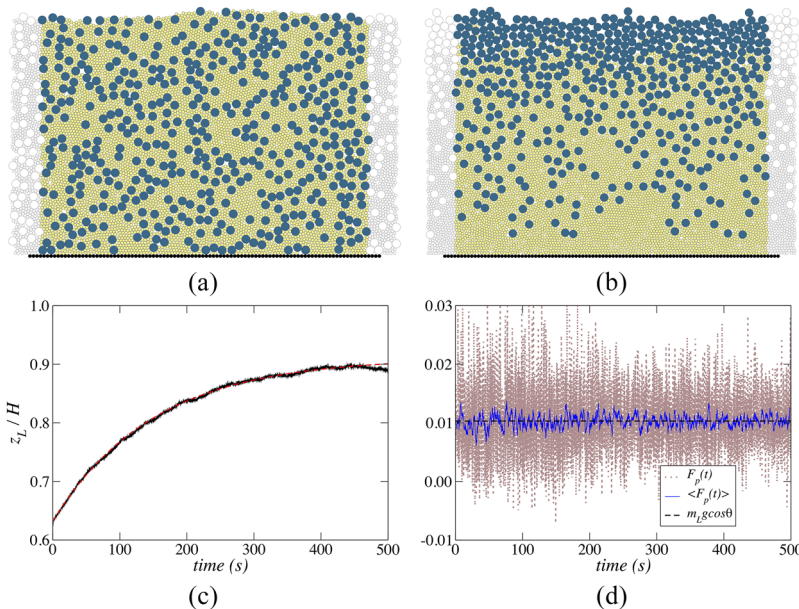

(c)   (d)

FIG. 5. Example of a mixture of smaller grains and larger grains such that $D/d = 3$ and $\Phi_L \simeq 0.4$ (a) in the initial state and (b) after segregation occurred due to flow under gravity at slope $\theta = 21.5°$; the position of the center of mass of the larger grains z_L is shown in the course of time in (c) (normalised by the flow thickness H). The dashed line shows an exponential fit. In (d), the instantaneous mean vertical force seen by large grains $F_p(t)$ is shown for all time steps (dotted line) and averaged over 25 time steps [$\langle F_p(t) \rangle$ full line]; the dashed line shows the weight of a large grain.

The rising dynamics may be described by the position of the centre of mass of the larger grains z_L and its evolution in the course of time [Fig. 5(c)]. As observed elsewhere,[15,24,35,38] the segregation is not complete, namely, few larger grains remain in the bulk as a result of diffusion and remixing.[47]

B. Resulting force on large grains

The instantaneous vertical force resultant seen by each large grain p at a given time t is simply given by the projection of the forces $\vec{f_p^\alpha}$ transmitted at each contact α involving p,

$$f_{z,p}(t) = \sum_{\alpha=1}^{n_p^\alpha} \vec{f_p^\alpha}(t).\vec{z}, \tag{6}$$

where n_p^α is the number of contacts in which the grain p is involved. An estimate of the instantaneous mean vertical force seen by large grains p is obtained by averaging $f_{z,p}(t)$ over all the large grains,

$$F_p(t) = \frac{1}{N_L} \sum_{p=1}^{N_L} f_{z,p}(t), \tag{7}$$

with N_L being the total number of large grains. Figure 5(d) shows an example of the large fluctuations exhibited by F_p in the course of time.

Averaging over the whole duration of the simulation, we compute the average vertical force resultant seen by each element of the phase of a large grain during the whole segregation process,

$$F_L = \frac{1}{N_t} \frac{1}{N_L} \sum_{t=1}^{N_t} \sum_{p=1}^{N_L} f_{z,p}(t) = \frac{1}{N_t} \sum_{t=1}^{N_t} F_p(t), \tag{8}$$

where N_t is the number of simulation time steps. We compute F_L for all 72 simulations with different composition Φ_L, different slope angle θ, and different size ratio D/d. The dependence of F_L (normalised by $m_s g \cos \theta$, $m_s = \rho \pi d^2 / 4$) with the size ratio D/d is shown in Fig. 6. We exactly recover

$$F_L = \cos \theta \rho \pi \frac{D^2}{4} g, \tag{9}$$

namely, on average, contact forces exactly balance the weight of the large grains. As for single intruders, we do not measure any net lift force.

On the other hand, larger grains are submitted to very important force fluctuations, as visible from Fig. 5(d). As for single intruders, we may suppose that the rising dynamics is dominated by these large force fluctuations, coupled with the asymmetry of the resistance to upward motion (toward the free surface) and downward motion (toward the bottom) described in Refs. 42–45. Accordingly, large positive force fluctuations induce upward jumps toward the free surface, without being counterweighted by "sinking episodes" when negative force fluctuations come into play.

C. Focusing on positive force fluctuations

Analyzing the rising motion of large grains is made difficult by the fact that grains do not move in a synchronised way, and while some move up, other may sink down. Nevertheless, we can suppose that the rising dynamics can be understood from the analysis of the positive contribution of the mean vertical force $F_p(t)$ seen by the phase of large grains. Hence, we compute

$$F_L^+ = \frac{\sum_{t=1}^{N_t} \mathcal{H}(F_p) F_p}{\sum_{t=1}^{N_t} \mathcal{H}(F_p)}, \tag{10}$$

where $\mathcal{H}$ is the Heaviside function and the summation is made over all the time steps t of the simulation. The value of F_L^+ is computed for all simulations with different composition Φ_L, different slope angle θ, and different size ratio D/d. From their analysis, a non-trivial dependence between F_L^+ and the size ratio D/d emerges. We observe the following form (Fig. 7):

$$\frac{F_L^+}{m_s g} \simeq \lambda \left(\frac{D}{d} \right)^a \cdot \left(\frac{\langle d \rangle}{d} \right)^b, \tag{11}$$

where $\langle d \rangle = \Phi_L D + (1 - \Phi_L) d$ is the mean grain diameter for the mixture. The proportionality coefficient λ and the exponents a and b vary with the slope θ, and their value is summarized in Table II.

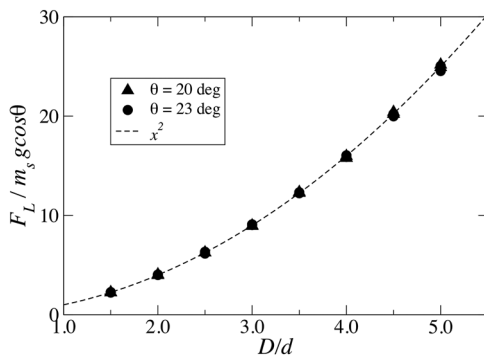The scaling (11) can be rearranged into a buoyancy-like force

FIG. 6. Mean time-averaged vertical force resultant on large grains F_L (normalised by the projected weight of a small grain $m_s g \cos \theta$) as a function of the normalised intruder diameter D/d for different slopes. We observe that on average, the vertical force exerted on the large grains exactly balances their weight.
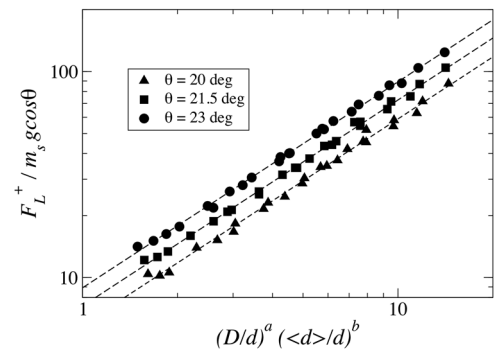

FIG. 7. Positive contribution of the vertical force resultant on the phase of large grains F_L^+ (normalised by the projected weight of a small grain $m_s g \cos \theta$) as a function of $(D/d)^a (\langle d \rangle / d)^b$, where a and b vary with the slope θ (see text for values). Dashed lines show linear fits.

TABLE II. Parameters for scaling (11).

Slope angle (deg)	λ	a	b	$c = 2 - (a + b)$
20	5.89	0.98	0.89	0.134
21.5	7.28	0.89	0.98	0.124
23	8.92	0.72	1.20	0.078

$$F_L^+ = \lambda \left(\frac{\langle d \rangle}{D}\right)^b . \left(\frac{d}{D}\right)^c \times \rho \pi \frac{D^2}{4} g, \qquad (12)$$

where b and $c = 2 - (a + b)$ are, respectively, of the order of 1 and 0.1 (see Table II for exact values). The pre-factor formed by $(\langle d \rangle/D)^b.(d/D)^c$ exhibits an explicit dependence on the composition through the mean grain diameter $\langle d \rangle = \Phi_L D + (1 - \Phi_L)d$. Accordingly, for a given grain size ratio, higher volume fractions of large grains favor large positive force fluctuations, hence presumably segregation. This holds at least in the range of volume fractions investigated; for larger values of ϕ_L, however, the scaling (12) is likely to break down, when smaller grains do no longer form a continuum but are trapped in the matrix of large grains.

V. DISCUSSION

Applying the contact dynamics method, we have performed discrete numerical simulations of segregating granular flows in the case of single free intruders and in the case of bi-disperse granular mixtures. In both configurations, while segregation occurs, we did not observe any measurable lift force acting on the larger grains. On the contrary, we observe that the large force fluctuations acting on the larger grains reduce to their weight, following the mere action-reaction principle.

Experiments consisting of plunging an intruder in a static granular bed or withdrawing it from an initially buried state report a strong asymmetry between the forces necessary to accomplish these two motions. In the work of Hill et al.,[42] forces necessary to withdraw a large intruder are about one order of magnitude smaller than the forces necessary to bury it (see Fig. 8). These results hold for different intruder sizes and shapes, different burying depths, and different container widths. This asymmetry was later corroborated by Schröter et al.[43] for rods (see Fig. 9) and by Martinez Carreaux[44] for spheres and rods, also reporting withdrawal forces at least
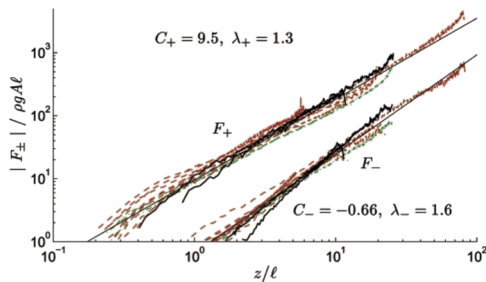
FIG. 8. Rescaled plots of the plunging forces, F+, and the withdrawal forces, F−, for horizontal rods in beds of monodisperse glass beads. Reproduced with permission from Hill et al., "Scaling vertical drag forces in granular media," Europhys. Lett. **72**(1), 137–143 (2005). Copyright 2005 EDP Sciences.
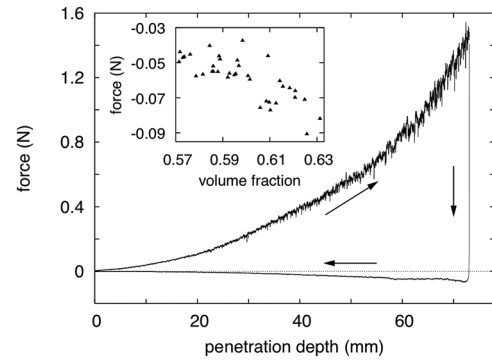
FIG. 9. Forces measured during a full cycle of insertion and withdrawal of an intruder in a granular bed at a volume fraction $\phi = 0.602$. Reproduced with permission from Schröter et al., "Phase transition in a static granular system," Europhys. Lett. **78**(4), 44004 (2007). Copyright 2007 Europhysics Letters.

10 times smaller than plunging forces. In the work of Li et al.,[45] similar results are reported and used to explain legged locomotion in sands.

This asymmetry is not surprising and reflects the difference of boundary conditions at the top and bottom of the granular container: while plunging requires pushing aside and rearranging grains whose motion will be opposed by a rigid wall, withdrawing motion is easily accommodated by the freely deforming free surface. It is however interesting that this effect persists at large depth, implying that the boundary condition formed by the free surface is felt throughout the system. As suggested in Ref. 42, we may suppose the existence of a cut-off depth at which the difference of forces between plunging and withdrawing will vanish, in a very large container. Meanwhile, such a (symmetrical) regime has not been observed yet.

Hence, any body buried in a granular flow and submitted to force fluctuations will meet a different resistance when subjected to upward or downward momentum and should logically rise as a result. We can try to quantify this effect using a very simple model, based on a frictional representation of the resistance to motion.[42,46] We suppose an intruder (of diameter D), buried in a dense granular flow at a depth $(H - z_I) \gg D$ and undergoing collisions with its smaller neighbours so that it alternatively gains momentum in the upward and downward directions, in a symmetrical way. The corresponding upward and downward motion is resisted by the work of friction forces $\mu_e P(z_I)D$, where μ_e is the effective coefficient of friction and $P(z_I) = \rho g(H - z_I)$ is the pressure at depth $(H - z_I)$. Following Refs. 42–45, the resistance to downward motion is larger than the resistance to upward motion; hence, we define two corresponding coefficients of friction $\mu_e^\downarrow$ and $\mu_e^\uparrow$ such that $\mu_e^\downarrow > \mu_e^\uparrow$. The energy gained during the collisions is entirely dissipated by the work of friction forces while the intruder moves upwards and downwards over $\Delta z^\uparrow$ and $\Delta z^\downarrow$, respectively. If we suppose the same amount of energy to be involved in upward and downward collisions, and if we moreover neglect the gain and loss of potential energy due to the intruder rising and sinking [justified by the fact that $D \ll (H - z_I)$], then $\mu_e^\uparrow \rho g(H - z_I)D\Delta z^\uparrow \simeq -\mu_e^\downarrow \rho g(H - z_I)D\Delta z^\downarrow$, and we simply obtain $\Delta z^\uparrow/\Delta z^\downarrow = -\mu_e^\downarrow/\mu_e^\uparrow$. If the ratio $\mu_e^\downarrow/\mu_e^\uparrow$ is of the order of 10 (as found in the literature), we immediately see how

upward motion is favored and how an intruder would rapidly end up reaching the free surface. The result is less spectacular if instead of considering the simplified form for the resisting forces $\mu_e \rho g (H - z_I) D$ we adopt the full dependence given in Ref. 42 for spheres, namely, $\mu_e^\uparrow \rho g (H - z_I)^{1.8} D^{-0.8} D$ for upward motion with $\mu_e^\uparrow = 1.2$ and $\mu_e^\downarrow \rho g (H - z_I)^{1.2} D^{-0.2} D$ for downward motion, with $\mu_e^\downarrow = 15$. In this case, for an intruder buried at a depth 40 times its diameter under the free surface (namely, the initial state in our simulations), we find $\Delta z^\uparrow / \Delta z^\downarrow \simeq 1.4$; this ratio increases while the intruder rises.

The studies by Hill *et al.*,[42] Schröter *et al.*,[43] Martinez Carreaux,[44] and Li *et al.*[45] were all considering static granular beds. Generalisation to granular flows hence requires additional work. In this case, the granular temperature induced by the shear is expected to decrease the overall resistance to motion, as reported in Ref. 49. Yet the geometrical asymmetry formed by the boundary condition remains so that the induced asymmetry on upward and downward resistance to bottom should not be suppressed.

Our results are also interesting in the perspective of understanding the role of temperature gradients in segregation processes.[23,25] In the work of Hill and Tan,[25] the gradients of kinetic stresses are introduced to explain the segregation dynamics in addition to the gradients of contact stresses considered in the model by Gray and Thornton.[16] Our simulations suggest indeed that force fluctuations are playing a greater role than the mean forces, following the idea of Ref. 25. The force fluctuations exhibit moreover an explicit dependence on the grain size. The asymmetry of the granular bed itself in terms of resistance to motion would be taken into account in the model by Gray and Thornton[16] and its adaptation by Hill and Tan[25] through the linear drag law and the corresponding drag coefficient, which could include a dependence on the grain vertical velocity (upward or downward).

Meanwhile, it is difficult to extrapolate our analysis to the case of very dilute flows, for which granular temperature gradients dominate the dynamics.[50–52] For very large agitation, we may even suppose that the effect described in Refs. 42–45 vanishes and that other factors will take over: contact properties, side walls, etc.[53,54] These cases are however beyond the scope of this paper.

In Ref. 44, plunging and withdrawing experiments were carried out while adding a weighting lid at the surface of the granular bed. The effect of this weighting lid is to impede grain rearrangements at the free surface. Accordingly, both withdrawing forces and plunging forces are greatly increased by its presence, yet the anisotropy of the resistance to motion in the upward and downward directions is preserved. Hence, segregation occurring in confined settings such as shear cells, as studied by Golick and Daniels,[55] does not contradict the line of argument developed in this paper. In Ref. 55, it is shown that increasing the pressure on the top lid results in a slower segregation process, which fits the observation by Martinez Carreaux of an increasing resistance to motion in the granular packing.

In a different manner, the larger grains which are first segregated in a flowing bi-disperse flow form a lid at the top of the mixture (see Fig. 5). Since the density of large and small grains is the same, this lid is not weighting. But because it involves larger grains and thus a lesser contact density (for geometrical reasons), we may suppose that it forms a less tractable free surface, thereby increasing the resistance to upward motion. If that was the case, this could partly explain why segregation saturates, leaving larger grains behind in the flow bulk. Rather than remixing, it could be that upward motion is increasingly difficult because of the lid of larger grains already covering the free surface. This would also account for the fact that segregation in three dimensions is much more efficient than in two dimensions since grains reaching the free surface are often redirected in a different area of the flow (forming levées for instance) and are not given the opportunity to form a lid.

Segregation processes are often described in terms of the smaller grains having more chances to fill in the gap opening in the flow due to shear deformation.[11] This is indeed what one sees when watching the progress of a large grain in a flow of smaller ones: space opening in the wake of the large grain and closing behind it so it seems squeezed out. We explain this mechanism by the fact that the large grain, submitted to large force fluctuations, is allowed to cut its way through the matrix of smaller grains in the upward direction, thus leaving an empty space behind, while the equivalent in the downward direction is not true. In addition to gravity, the existence of two different boundary conditions formed by the free surface and the rigid bottom explains this difference of resistance to motion in the upward and downward directions.[42,44] In this respect, the mechanism allowing the rising dynamics of larger grains in granular flows is the same as that allowing legged locomotion in sand[45] and bears little resemblance with its hydrodynamical counterpart.

ACKNOWLEDGMENTS

[1]N. Casagli, L. Ermini, and G. Rosati, "Determining grain size distribution of the material composing landslide dams in the Northern Apennines: Sampling and processing methods," Eng. Geol. **69**, 83–97 (2003).

[2]N. K. Mitani, H. G. Matuttis, and T. Kadono, "Density and size segregation in deposits of pyroclastic flow," Geophys. Res. Lett. **31**, L15606, https://doi.org/10.1029/2004gl020117 (2004).

[3]B. Marks and I. Einav, "A mixture of crushing and segregation: The complexity of grainsize in natural granular flows," Geophys. Res. Lett. **42**, 274, https://doi.org/10.1002/2014gl062470 (2015).

[4]T. de Haas, L. Braat, J. R. F. W. Leuven, I. R. Lokhorst, and M. G. Kleinhans, "Effects of debris flow composition on runout, depositional mechanisms, and deposit morphology in laboratory experiments," J. Geophys. Res.: Earth Surf. **120**, 1949, https://doi.org/10.1002/2015JF003525 (2015).

[5]X. Wang, Z. Dong, J. Zhang, J. Qua, and A. Zhao, "Grain size characteristics of dune sands in the central Taklimakan Sand Sea," Sediment. Geol. **161**, 1–14 (2003).

[6]G. Félix and N. Thomas, "Relation between dry granular flow regimes and morphology of deposits: Formation of levées in pyroclastic deposits," Earth Planet. Sci. Lett. **221**, 197–213 (2004).

[7]C. Goujon, B. Dalloz-Dubrujeaud, and N. Thomas, "Bidisperse granular avalanches on inclined planes: A rich variety of behaviors," Eur. Phys. J. E **23**, 199–215 (2007).

[8]F. Moro, T. Faug, H. Bellot, and F. Ousset, "Large mobility of dry snow avalanches: Insights from small-scale laboratory tests on granular avalanches of bidisperse materials," Cold Reg. Sci. Technol. **62**, 55–66 (2010).

[9]C. G. Johnson, B. P. Kokelaar, R. M. Iverson, M. Logan, R. G. LaHusen, and J. M. N. T. Gray, "Grain-size segregation and levee formation in geophysical mass flows," J. Geophys. Res.: Earth Surf. **117**, F01032, https://doi.org/10.1029/2011jf002185 (2012).

[10]J. Bridgewater, W. S. Foo, and D. J. Stephens, "Particle mixing and segregation in failure zones—Theory and experiment," Powder Technol. **41**, 147–158 (1985).

[11]S. B. Savage and C. K. K. Lun, "Particle size segregation in inclined chute flow of dry cohesionless granular solids," J. Fluid Mech. **189**, 311–335 (1988).

[12]G. Berton, R. Delannay, P. Richard, N. Taberlet, and A. Valance, "Two-dimensional inclined chute flows: Transverse motion and segregation," Phys. Rev. E **68**, 051303 (2003).

[13]M. Schröter, S. Ulrich, J. Kreft, J. B. Swift, and H. L. Swinney, "Mechanisms in the size segregation of a binary granular mixture," Phys. Rev. E **74**, 011307 (2006).

[14]K. van der Vaart, P. Gajjar, G. Epely-Chauvin, N. Andreini, J. M. N. T. Gray, and C. Ancey, "Underlying asymmetry within particle size segregation," Phys. Rev. Lett. **114**, 238001 (2015).

[15]L. Jing, C. Y. Kwok, and Y. F. Leung, "Micro-mechanical origin of particle size segregation," Phys. Rev. Lett. **118**, 118001 (2017).

[16]J. M. N. T. Gray and A. R. Thornton, "A theory for particle size segregation in shallow granular free-surface flows," Proc. R. Soc. A **461**, 1447–1473 (2005).

[17]F. Radjai, M. Jean, J.-J. Moreau, and S. Roux, "Force distribution in dense two-dimensional granular systems," Phys. Rev. Lett. **77**(2), 274 (1996).

[18]T. S. Majmudar and R. P. Behringer, "Contact force measurements and stress-induced anisotropy in granular materials," Nature **435**, 1079 (2005).

[19]C. Voivret, F. Radjai, J.-Y. Delenne, and M. S. El Youssoufi, "Multiscale force networks in highly polydisperse granular media," Phys. Rev. Lett. **102**, 178001 (2009).

[20]J. M. N. T. Gray and B. P. Kokelaar, "Large particle segregation, transport and accumulation in granular free-surface flows," J. Fluid Mech. **652**, 105–137 (2010).

[21]P. Gajjar and J. M. N. T. Gray, "Asymmetric flux models for particle-size segregation in granular avalanches," J. Fluid Mech. **757**, 297–329 (2014).

[22]J. M. N. T Gray, "Particle segregation in dense granular flows," Annu. Rev. Fluid. Mech. **50**, 407–433 (2018).

[23]Y. Fan and K. M. Hill, "Theory for shear-induced segregation of dense granular mixtures," New J. Phys. **13**, 095009 (2011).

[24]T. Weinhart, S. Luding, and A. R. Thornton, "From discrete particles to continuum fields in mixtures," AIP Conf. Proc. **1542**, 1202–1205 (2013).

[25]K. M. Hill and D. S. Tan, "Segregation in dense sheared flows: Gravity, temperature gradients, and stress partitioning," J. Fluid Mech. **756**, 54–88 (2014).

[26]L. Staron and J. C. Phillips, "Stress partition and micro-structure in size-segregating granular," Phys. Rev. E **92**, 022210 (2015).

[27]M. Larcher and J. T. Jenkins, "Segregation and mixture profiles in dense, inclined flows of two types of spheres," Phys. Fluids **25**, 113301 (2013).

[28]Y. Ding, N. Gravish, and D. Goldman, "Drag induced lift in granular media," Phys. Rev. Lett. **106**, 028001 (2011).

[29]F. Q. Potiguar and Y. Ding, "Lift and drag in intruders moving through hydrostatic granular media at high speeds," Phys. Rev. E **88**, 012204 (2013).

[30]F. Guillard, Y. Forterre, and O. Pouliquen, "Depth-independent drag force induced by stirring in granular media," Phys. Rev. Lett. **110**, 138303 (2013).

[31]F. Guillard, Y. Forterre, and O. Pouliquen, "Lift forces in granular media," Phys. Fluids **26**, 043301 (2014).

[32]F. Guillard, Y. Forterre, and O. Pouliquen, "Scaling laws for segregation forces in dense sheared granular flows," J. Fluid Mech. **807**, 1–11 (2016).

[33]K. van der Vaart, M. P. van Schrojenstein Lantman, T. Weinhart, S. Luding, C. Ancey, and A. R. Thornton, "Segregation of large particles in dense granular flows suggests a granular Saffman effect," Phys. Rev. Fluids **3**, 074303 (2018).

[34]P. G. Rognon, J.-N. Roux, M. Naaim, and F. Chevoir, "Dense flows of bidisperse assemblies of disks down an inclined plane," Phys. Fluids **19**, 058101-1 (2007).

[35]A. R. Thornton, T. Weinhart, S. Luding, and O. Bokhove, "Modeling of particle size segregation: Calibration using the discrete particle method," Int. J. Mod. Phys. C **23**, 1240014 (2012).

[36]B. Marks, P. Rognon, and I. Einav, "Grainsize dynamics of polydisperse granular segregation down inclined planes," J. Fluid Mech. **690**, 499–511 (2012).

[37]D. R. Tunuguntla, O. Bokhove, and A. R. Thornton, "A mixture theory for size and density segregation in shallow granular free-surface flows," J. Fluid Mech. **749**, 99–112 (2014).

[38]L. Staron and J. C. Phillips, "Segregation time-scales in bi-disperse granular flows," Phys. Fluids **26**(3), 033302 (2014).

[39]D. R. Tunuguntla, T. Weinhart, and A. R. Thornton, "Comparing and contrasting size-based particle segregation models," Comput. Part. Mech. **4**, 387–405 (2017).

[40]M. Jean and J.-J. Moreau, "Unilaterality and dry friction in the dynamics of rigid bodies collections," in *Proceedings of Contact Mechanics International Symposium*, edited by A. Curnier (Presses Polytechniques et Universitaires Romandes, Lausanne, 1992), pp. 31–48.

[41]J.-J. Moreau, "Some numerical methods in multibody dynamics: Application to granular materials," Eur. J. Mech.: A/Solids **13**(4), 93–114 (1994).

[42]G. Hill, S. Yeung, and S. A. Koelher, "Scaling vertical drag forces in granular media," Europhys. Lett. **72**(1), 137–143 (2005).

[43]M. Schröter, S. Nägle, C. Radin, and H. L. Swinney, "Phase transition in a static granular system," Europhys. Lett. **78**(4), 44004 (2007).

[44]F. J. Martinez Carreaux, Force de résistance au mouvement d'un objet dans un milieu granulaire, Université Paris Sud - Paris XI, 2013. NNT: 2013PA112345, tel-00968674 (2013), https://tel.archives-ouvertes.fr/tel-00968674.

[45]C. Li, T. Zhang, and D. I. Goldman, "A terradynamics of legged locomotion on granular media," Science **339**, 1408–1412 (2013).

[46]Z. Peng, X. Xu, K. Lu, and M. Hou, "Depth dependence of vertical plunging force in granular medium," Phys. Rev. E **80**, 021301 (2009).

[47]J. M. N. T. Gray and V. A. Chugunov, "Particle-size segregation and diffusive remixing in shallow granular avalanches," J. Fluid Mech. **569**, 365–398 (2006).

[48]A. Tripathi and D. V. Khakhar, "Numerical simulation of the sedimentation of a sphere in a sheared granular fluid: A granular Stokes experiment," Phys. Rev. Lett. **107**(10), 108001 (2011).

[49]G. A. Caballero-Robledo and E. Clément, "Rheology of a sonofluidized granular packing," Eur. Phys. J. E **30**, 395 (2009).

[50]A. Seguin, Y. Bertho, P. Gondret, and J. Crassous, "Dense granular flow around a penetrating object: Experiment and hydrodynamic model," Phys. Rev. Lett. **107**, 048001 (2011).

[51]J. T. Jenkins and D. K. Yoon, "Segregation in binary mixtures under gravity," Phys. Rev. Lett. **88**, 194301 (2002).

[52]M. Larcher and J. T. Jenkins, "The evolution of segregation in dense inclined flows of binary mixtures of spheres," J. Fluid Mech. **782**, 405–429 (2015).

[53]S. Ulrich, M. Schröter, and H. L. Swinney, "Influence of friction on granular segregation," Phys. Rev. E **76**, 042301 (2007).

[54]S. Yang, Y. Sun, L. Zhang, and J. Wei Chew, "Numerical study on the axial segregation dynamics of a binary-size granular mixture in a three-dimensional rotating drum," Phys. Fluids **29**, 103302 (2017).

[55]L. A. Golick and K. E. Daniels, "Mixing and segregation rates in sheared granular materials," Phys. Rev. E **80**, 042301 (2009).